

# On inverse doping profile problems for the stationary voltage–current map

A Leitão<sup>1</sup>, P A Markowich<sup>2</sup> and J P Zubelli<sup>3</sup>

<sup>1</sup> Department of Mathematics, Federal University of St Catarina, 88040-900 Florianopolis, Brazil

<sup>2</sup> Department of Mathematics, University of Vienna, Boltzmanngasse 9, A-1090 Vienna, Austria

<sup>3</sup> IMPA, Estr. Dona Castorina 110, 22460-320 Rio de Janeiro, Brazil

E-mail: [aleitao@mtm.ufsc.br](mailto:aleitao@mtm.ufsc.br), [peter.markowich@univie.ac.at](mailto:peter.markowich@univie.ac.at) and [zubelli@impa.br](mailto:zubelli@impa.br)

Received 4 February 2006, in final form 11 April 2006

Published 19 May 2006

Online at [stacks.iop.org/IP/22/1071](http://stacks.iop.org/IP/22/1071)

## Abstract

We consider the problem of identifying possibly discontinuous doping profiles in semiconductor devices from data obtained by stationary voltage–current maps. In particular, we focus on the so-called *unipolar case*, a system of PDEs derived directly from the drift diffusion equations. The related inverse problem corresponds to an inverse conductivity problem with partial data. The identification issue for this inverse problem is considered. In particular, for a discretized version of the problem, we derive a result connected to diffusion tomography theory. A numerical approach for the identification problem using level set methods is presented. Our method is compared with previous results in the literature, where Landweber–Kaczmarz-type methods were used to solve a similar problem.

(Some figures in this article are in colour only in the electronic version)

## 1. Introduction

The precise implantation of the doping profile is crucial for the desired performance of semiconductor devices. In many applications, there is substantial interest in replacing expensive laboratory testing by numerical simulation and non-destructive testing, in order to minimize the manufacturing costs of semiconductors as well as for quality control. The identification of the doping profile from indirect measurements is called an inverse doping profile problem. In laboratory experiments, there are different types of measurement techniques, such as *laser-beam-induced current* (LBIC) [11–13], *capacitance* [4, 5] and *current flow* [4, 6] measurements. These measurement techniques are related to different types of data and lead to various inverse doping problems. This paper is devoted to the analysis of an identification problem related to a particular model, the so-called *unipolar system*, derived from the stationary drift diffusion equations under certain simplifying assumptions on the

concentration of free carriers of positive charges and on the recombination–generation rate. In this framework, the parameter function to be identified is the *doping profile*. It depends on the space variables only and represents the doping concentration, which gives the performance of the device. It is produced by diffusion of different materials into the silicon crystal and by implantation with an ion beam.

We shall focus on reconstruction problems based on data generated by the *voltage–current* ( $V$ – $C$ ) map, i.e., an operator that takes the applied voltage at a specified boundary part (corresponding to a semiconductor contact) into the outflow current density on a different boundary part (another contact). The two main contributions of this paper consist of a theoretical identification result for a discretized version and the analysis of a level set type method for solving the inverse doping profile problem in the unipolar case.

The starting point of the mathematical model discussed in this paper is the system of *stationary drift diffusion equations* (see system (1)). This system of equations, derived more than 50 year ago [28], is most widely used to describe semiconductor devices and represents an accurate compromise between efficient numerical solvability of the mathematical model and realistic description of the underlying physics [22, 23, 26].

This paper is organized as follows. In section 2, we briefly introduce the *drift diffusion* equations, the  $V$ – $C$  map and the *stationary linearized unipolar system*. The latter models the direct problem related to the inverse doping profile problem analysed in this paper.

In section 3, we treat the identification issue for this inverse problem. We do not have, at present, a theoretical result showing uniqueness in the identification of the doping profile. However, we do present two lines of reasoning that support the conjecture of an identifiability result for the doping profile: the first one is based on recent results due to Bukhgeim and Uhlmann [3] on global uniqueness for the local Dirichlet-to-Neumann map and the second one concerns a discretized version of the problem that falls within the scope of tomography in the presence of diffusion and scattering [16, 17].

In section 4, we use a level set type method to reconstruct the doping profile function. In this approach, a single pair of voltage–current data is used. We compare our results with the competing Landweber–Kaczmarz method used in [4] to solve a similar problem. An analytical result concerning stability, convergence and well posedness of this level set method is also presented. Section 5 is devoted to final comments and conclusions.

## 2. Inverse doping profile problems

### 2.1. The semiconductor equations

The *drift diffusion* system of equations is the most widely used model to describe semiconductor devices. The mathematical modelling of semiconductor equations has developed significantly, together with their manufacturing. The *basic semiconductor device equations* were first presented, in the level of completeness discussed here, by van Roosbroeck in [28]. Since then, it has been subject of intensive mathematical and numerical investigation. Recent detailed expositions of the subject of modelling, analysis and simulation of semiconductor equations can be found in [22, 23, 26] to cite a few.

For the sake of simplicity, we formulate the drift diffusion equations in terms of the *slotboom variables* ( $u$ ,  $v$ ). Using an adequate change of variables, motivated by the Einstein relations, the functions  $u$  and  $v$  are obtained from the electron density function and the hole density function, respectively. The details concerning the derivation of the model below can be found in [4, 5].

The stationary drift diffusion equations consist of the Poisson equation (1a) for the (rescaled) electrostatic potential  $V$  and the continuity equations (1b) and (1c).

$$\lambda^2 \Delta V = \delta^2 (e^V u - e^{-V} v) - C \quad \text{in } \Omega, \tag{1a}$$

$$\operatorname{div} J_n = \delta^4 Q(V, u, v, x)(uv - 1) \quad \text{in } \Omega, \tag{1b}$$

$$\operatorname{div} J_p = -\delta^4 Q(V, u, v, x)(uv - 1) \quad \text{in } \Omega, \tag{1c}$$

$$V = V_D := U + V_{\text{bi}} \quad \text{on } \partial\Omega_D, \tag{1d}$$

$$u = u_D := e^{-U} \quad \text{on } \partial\Omega_D, \tag{1e}$$

$$v = v_D := e^U \quad \text{on } \partial\Omega_D, \tag{1f}$$

$$\nabla V \cdot \nu = J_n \cdot \nu = J_p \cdot \nu = 0 \quad \text{on } \partial\Omega_N, \tag{1g}$$

where the densities of the electron and hole currents  $J_n$  and  $J_p$  satisfy the current relations:

$$J_n = \mu_n q n_i e^V \nabla u \quad \text{and} \quad J_p = -\mu_p q n_i e^{-V} \nabla v.$$

Here the positive constants  $q$  and  $n_i$  denote the elementary charge and the intrinsic charge density, respectively. Moreover,  $\mu_n$  and  $\mu_p$  represent the (rescaled) mobilities of electrons and holes, respectively.

The domain  $\Omega \subset \mathbb{R}^d$  ( $d = 2, 3$ ) represents the semiconductor device. Two dimensionless positive parameters occur, namely  $\lambda$  and  $\delta$ , both small in many practical applications. The function  $Q$  is defined implicitly by the recombination–generation rate function. As far as boundary conditions are concerned, the function  $U$  is the applied potential and  $V_{\text{bi}}(x) := U_T \ln(n_D(x)/n_i)$ , where  $U_T$  is the thermal voltage.

The function  $C = C(x)$  denotes the doping concentration, which is produced by diffusion of different materials into the silicon crystal and by implantation with an ion beam. In many technological applications, the *doping profile*  $C$  is the parameter that has to be identified. Because of inaccuracies in the manufacturing process, semiconductor devices should pass through some testing to ensure high quality. The inverse problem we are concerned with is related to a non-destructive identification procedure, based on experiments modelled by the *voltage-to-current* operator.

In the following, we briefly discuss the boundary conditions (1d)–(1g). The boundary of  $\Omega$  is assumed to be divided into two nonempty parts:  $\partial\Omega = \partial\Omega_N \cup \partial\Omega_D$ . The segments of  $\partial\Omega_D$  correspond to the semiconductor contacts, where Dirichlet boundary conditions are prescribed. Differences in  $U$  between different parts of  $\partial\Omega_D$  correspond to the applied bias between these two contacts. The Neumann part of the boundary  $\partial\Omega_N = \partial\Omega - \partial\Omega_D$  models insulating or artificial surfaces. Therefore, a zero current flow and a zero electric field in the normal direction are prescribed.

Existence (in the weak sense) and some uniqueness results for system (1) can be found in [22, 23]. Under suitable regularity assumptions on the boundary conditions  $u_D, v_D, U$  and on the doping profile  $C$ , one can prove that system (1) admits a weak solution  $(V, u, v)$  in  $(H^1(\Omega) \cap L^\infty(\Omega))^3$ . See [23, theorem 3.3.16] and [5, theorem 4.2]. Stronger existence results for  $(H^2(\Omega) \cap L^\infty(\Omega))^3$  can be found in [22].

### 2.2. The inverse problem

We start the discussion by introducing the *voltage–current* ( $V$ – $C$ ) map:

$$\begin{aligned} \Sigma_C &: H^{3/2}(\partial\Omega_D) \rightarrow L^2(\Gamma_1) \\ U &\mapsto J \cdot \nu|_{\Gamma_1} = (J_n + J_p) \cdot \nu|_{\Gamma_1}, \end{aligned}$$

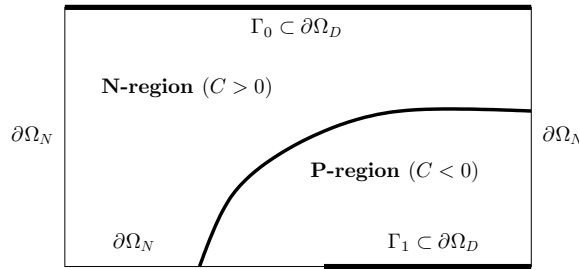


**Figure 1.** The domain  $\Omega \subset \mathbb{R}^2$  represents a P–N diode. The P-region corresponds to the subregion of  $\Omega$ , where  $C < 0$ . In the N-region,  $C > 0$  holds. The curve between these regions is called the P–N junction.

where  $\Gamma_1 \subset \partial\Omega_D$  corresponds to the part of the boundary (a contact) where measurements are taken. Note that the map  $\Sigma_C$  takes the applied voltage  $U$  into the corresponding current density. In the inverse problem considered in this paper, the linearized  $V$ – $C$  map at  $U = 0$  plays a key role, as we shall see later in this section.

Since the potential can be shifted by a constant, we shall assume without loss of generality that  $U(x)|_{\Gamma_1} = 0$ . In practical applications, the applied potential  $U \in H^{3/2}(\partial\Omega_D)$  is assumed to be piecewise constant in the contacts. To illustrate, a very simple semiconductor device is shown in figure 1.

In the next lemma, we briefly review some properties of the nonlinear operator  $\Sigma_C$ . A complete proof can be found in [5].

**Lemma 2.1.** *The current  $\Sigma_C(U) \in L^2(\Gamma_1)$  is uniquely defined for each voltage  $U \in H^{3/2}(\partial\Omega_D)$  in the neighbourhood of  $U = 0$ , i.e., the operator  $\Sigma_C$  is well defined in the neighbourhood of  $U = 0$ . Moreover,  $\Sigma_C$  is continuous and continuously Fréchet differentiable in the neighbourhood of  $U = 0$ .*

If  $U = 0$ , the solution of (1) is given by  $(V, u, v) = (V^0, 1, 1)$ , where  $V^0$  is a solution of the Poisson equation at equilibrium

$$\begin{cases} \lambda^2 \Delta V^0 = \delta^2 (e^{V^0} - e^{-V^0}) - C & \text{in } \Omega, \\ V^0 = V_{bi} & \text{on } \partial\Omega_D, \\ \nabla V^0 \cdot \nu = 0 & \text{on } \partial\Omega_N. \end{cases} \tag{2}$$

From now on, the following simplifying assumptions are made.

- (A1) The concentration of holes satisfies  $v = 0$ .
- (A2) No recombination–generation rate is present, i.e.,  $Q = 0$ .
- (A3) The electron mobility is constant ( $\mu_n = 1$ ) and  $q = 1$ .

Under these assumptions, we conclude that the Gateaux derivative of  $\Sigma_C$  at  $U = 0$  in the direction  $h \in H^{3/2}(\partial\Omega_D)$  is given by

$$\Sigma'_C(0)h = e^{V^0} \hat{u}_v|_{\Gamma_1},$$

where  $\hat{u}$  and  $V^0$  solve

$$\begin{cases} \operatorname{div}(e^{V^0} \nabla \hat{u}) = 0 & \text{in } \Omega, \\ \hat{u} = h & \text{on } \partial\Omega_D, \\ J_n \cdot \nu = 0 & \text{on } \partial\Omega_N, \end{cases} \quad \begin{cases} \lambda^2 \Delta V^0 = e^{V^0} - C & \text{in } \Omega, \\ V^0 = V_{bi} & \text{on } \partial\Omega_D, \\ \nabla V^0 \cdot \nu = 0 & \text{on } \partial\Omega_N. \end{cases} \tag{3}$$

The decoupled system (3) is called the *stationary linearized unipolar case (close to equilibrium)*. The inverse problem of identifying the doping profile in system (3) corresponds to the identification of  $C(x)$  from the *parameter-to-output map*

$$F : D(F) \subset L^2(\Omega) \rightarrow \mathcal{L}(H^{3/2}(\partial\Omega_D); H^{1/2}(\Gamma_1))$$

$$C \mapsto \Sigma'_C(0).$$

Since  $\mu_n = 1$  and  $V = V_{bi}(x)$  is known at  $\partial\Omega_D$ , the measured current data  $J_n \cdot \nu = \mu_n e^{V^0} \hat{u}_\nu$  at  $\Gamma_1$  can be directly replaced by the Neumann data  $\hat{u}_\nu$ . Therefore, the inverse problem can be divided into two distinct steps.

**Identification problem 2.2** (stationary linearized unipolar case).

- (1) Define  $\gamma := e^{V^0}$  and identify  $\gamma$  from the Dirichlet-to-Neumann (DtN) map  $\Lambda_\gamma : U \mapsto \gamma \hat{u}_\nu|_{\Gamma_1}$ , where  $\hat{u}$  solves

$$\operatorname{div}(\gamma \nabla \hat{u}) = 0 \quad \text{in } \Omega, \quad \hat{u} = U \quad \text{on } \partial\Omega_D, \quad \hat{u}_\nu = 0 \quad \text{on } \partial\Omega_N.$$

- (2) Obtain the doping profile  $C$  from  $C(x) = \gamma(x) - \lambda^2 \Delta(\ln \gamma(x))$ ,  $x \in \Omega$ .

The evaluation of  $C$  from  $\gamma$  can be explicitly performed (a direct problem) and is a standard procedure. The identification issue in problem 2.2 (1) corresponds to the *electrical impedance tomography* in elliptic equations with mixed boundary data. For the case of the full DtN operator, i.e.,  $\Gamma_1 = \partial\Omega_D = \partial\Omega$ , this inverse problem has been intensively analysed in the literature (see e.g. [2, 19] for a survey).

**3. Inverse doping profile: identification issue**

In this section, we consider some theoretical aspects of the inverse doping profile problem. Despite the encouraging numerical results of section 4, at present, we do not have a theoretical result showing uniqueness of the doping profile from  $V$ – $C$  data measured on distinct subdomains of the boundary. In subsection 3.1, we present the state of the art that comes closest to the identifiability question related to problem 2.2 (1). This approach is based on recent results due to Bukhgeim and Uhlmann [3] on global uniqueness for the local Dirichlet-to-Neumann map. In the last subsection, we present a reasoning that supports the conjecture of an identifiability result for the doping profile. It concerns a discretized version of the problem that falls within the scope of identifying the potential of a discretized Schrödinger equation using external measurements. We treat this problem using techniques from the so-called isotropic case of diffuse tomography [16, 17].

*3.1. Global uniqueness approach*

In the following, we consider  $\Omega$  to be two dimensional, unless stated otherwise. Therefore, each current measurement is given by a function of one space variable defined on  $\Gamma_1 \subset \partial\Omega$ . Obviously, a single measurement is not sufficient to identify the doping profile  $C : \Omega \subset \mathbb{R}^2 \rightarrow \mathbb{R}$ . However, adapting some results from [24], related to electrical impedance tomography, we argue in the full data case that the knowledge of the operator  $F$  in subsection 2.2 is enough to determine  $C$  uniquely.

We reason as follows: let  $V^0$  be the solution of the Poisson equation at equilibrium in (3). Given an input voltage  $U \in H^{3/2}(\partial\Omega_D)$ , the output current can be identified (after rescaling) with the Neumann data of  $u$  at  $\Gamma_1$ , i.e.,  $u_\nu|_{\Gamma_1} = \Lambda_C(U)$ , where  $u$  is the solution of the elliptic equation in (3). From standard results in elliptic theory, one concludes that for a domain  $\Omega$

with Lipschitz boundary, there is a one-to-one relation between the solutions  $V^0 \in H^2(\Omega)$  of the Poisson equation and the potentials  $C \in L^2(\Omega)$ . Therefore, it is enough to consider the problem of identifying the potential  $V^0$  in (3) or, equivalently, the conductivity  $\gamma = e^{V^0}$  as stated in problem 2.2.

The problem of identifying conductivities from the DtN map was analysed by Nachman in [24]. Adapting his result to identification problem 2.2 one can prove that for a bounded  $\Omega \subset \mathbb{R}^2$  with Lipschitz boundary,  $\Gamma_1 = \partial\Omega_D = \partial\Omega$  and  $C_1, C_2$ , two doping profiles such that the corresponding conductivities satisfy

$$\gamma_1, \gamma_2 \in D(F) := \{\gamma \in W^{2,p}(\Omega), p > 1; \gamma_+ \geq \gamma(x) \geq \gamma_- > 0 \text{ a.e. in } \Omega\},$$

the equality  $\Lambda_{\gamma_1} = \Lambda_{\gamma_2}$  implies  $C_1 = C_2$ .

This result of Nachman has been recently improved by Astala and Päiväranta [1], who proved that any  $L^\infty$  conductivity in two dimensions can be determined uniquely from the DtN map.

We address yet another identification result (for the inverse doping profile problem) based on the global uniqueness approach. Concerning uniqueness results for the DtN operator with partial boundary data, this result corresponds to the state of the art. Let  $\Omega \subset \mathbb{R}^n$ , with  $n \geq 3$ , be a bounded domain with  $C^2$  boundary. Further, let  $\xi \in \mathbb{R}^n$  with  $\|\xi\| = 1$  and  $\varepsilon > 0$  be given. We define

$$\Gamma_0 := \{x \in \partial\Omega; \langle \nu(x), \xi \rangle > -\varepsilon\}, \quad \Gamma_1 := \{x \in \partial\Omega; \langle \nu(x), \xi \rangle < \varepsilon\},$$

where  $\nu(x)$  is the unit normal vector at  $x \in \partial\Omega$  (note that  $\Gamma_0 \cap \Gamma_1 \neq \emptyset$ ). Moreover, let  $C_1, C_2$  be doping profiles such that the corresponding conductivities satisfy  $\gamma_1, \gamma_2 \in C^2(\overline{\Omega})$  and  $\gamma_j(x) \geq \gamma_- > 0$  a.e. in  $\Omega$ ,  $j = 1, 2$ . Then, the equality  $\Lambda_{\gamma_1} = \Lambda_{\gamma_2}$  implies  $C_1 = C_2$  (see [3]).

Note that this result applies to three-dimensional domains  $\Omega$  with regular boundary and, moreover,  $\partial\Omega = \partial\Omega_D = \Gamma_0 \cup \Gamma_1$ ,  $\Gamma_0 \cap \Gamma_1 \neq \emptyset$ , i.e., the contacts where the voltage is prescribed ( $\Gamma_0$ ) and where the current is measured ( $\Gamma_1$ ) overlap.

### 3.2. The discrete Schrödinger equation with partial DtN data

In this section, we consider the characterization problem for the Schrödinger operator potential  $V$  given partial information on the Dirichlet-to-Neumann map  $\Lambda^V$  associated with the problem

$$\begin{cases} -\Delta w + Vw = 0 & \text{in } \Omega, \\ w|_{\partial\Omega} = \phi. \end{cases} \quad (4)$$

It is well known that the change of variables

$$w = \gamma^{1/2}u \quad \text{and} \quad V = \gamma^{-1/2}\Delta\gamma^{1/2} \quad (5)$$

establishes a one-to-one correspondence between the solutions of (4) and those of

$$\begin{cases} \operatorname{div}(\gamma\nabla u) = 0 & \text{in } \Omega, \\ u|_{\partial\Omega} = \gamma^{-1/2}|_{\partial\Omega}\phi. \end{cases} \quad (6)$$

The Dirichlet-to-Neumann map for (4) is related to that of (6) by

$$\Lambda^V(\phi) = \gamma^{-1/2}\Lambda_\gamma(\gamma^{-1/2}\phi) + \frac{1}{2\gamma}\frac{\partial\gamma}{\partial n}\phi. \quad (7)$$

It is clear that the knowledge of the DtN map  $\Lambda^V$  for equation (4) is equivalent to the knowledge of its counterpart  $\Lambda_\gamma$  for (6). Furthermore, any restriction of  $\Lambda^V$  to  $\phi$  supported

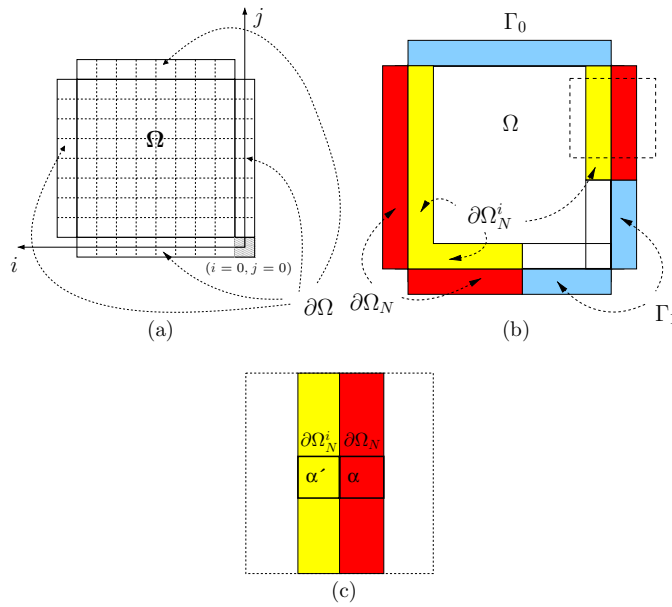


**Figure 2.** Picture (a) shows the discretized region  $\Omega$  under consideration and its boundary  $\partial\Omega$ . It also shows the origin  $(0, 0)$  on the bottom-right corner. In picture (b), the boundary parts  $\partial\Omega_N, \partial\Omega_D = \Gamma_0 \cup \Gamma_1$  are shown. Picture (c) zooms in the squared region marked in (b). It shows the boundary  $\partial\Omega_N$  and its adjacent interior part  $\partial\Omega_N^i$ .

on a subset  $\Gamma_0$  of the boundary corresponds to the restriction of  $\Lambda_\gamma$  supported on this set  $\Gamma_0$ . If we consider current measurements taken in a subset  $\Gamma_1$  contained in  $\partial\Omega$ , then at the level of  $\Lambda^V$  this means that we will only consider the information from  $\Lambda^V$  on  $\Gamma_1$ . Let us call such a map  $\Lambda^V|_{\Gamma_0, \Gamma_1}$ .

To the best of our knowledge, there is no characterization result of  $V$  based on  $\Lambda^V|_{(\Gamma_0, \Gamma_1)}$  when  $\Gamma_0 \cap \Gamma_1 = \emptyset$ . We explore here the discrete analogue of the Dirichlet-to-Neumann characterization problem with partial data for the Schrödinger operator. In this context, we consider a discretization  $V_{ij} = V(x_i, y_j)$  of  $V : \Omega \rightarrow \mathbb{R}$  for  $(i, j) \in \Omega \stackrel{\text{def}}{=} \{(i, j) | 1 \leq i, j \leq N, i, j \in \mathbb{Z}\}$ . For a mesh size  $\Delta x = \Delta y = \epsilon$ , the first equation in (4) is replaced by

$$u_{ij} = \frac{1}{4 + \epsilon^2 V_{ij}} (u_{i+1, j} + u_{i-1, j} + u_{i, j+1} + u_{i, j-1}) \quad \text{for } (i, j) \in \Omega. \quad (8)$$

We define  $w_{ij} = 4/(4 + \epsilon^2 V_{ij})$  and consider the set of equations described by

$$u_{ij} - \frac{w_{ij}}{4} (u_{i+1, j} + u_{i-1, j} + u_{i, j+1} + u_{i, j-1}) = 0, \quad \text{where } (i, j) \in \Omega. \quad (9)$$

We remark that except for minor modifications, in what follows, we could use  $1 \leq i \leq N_1$  and  $1 \leq j \leq N_2$  (see figure 2).

The system of equations defined by (9) must be supplemented with suitable boundary conditions. In [16, 17], Dirichlet-type boundary conditions were imposed for  $u_{i, j}$  whenever  $(i, j) \in \partial\Omega$ , where  $\partial\Omega$  is the set of points  $(i, j)$  with  $0 \leq i, j \leq N + 1$  where either  $i \in \{0, N + 1\}$  or  $j \in \{0, N + 1\}$ , but not both. See figure 2. More precisely, in [16, 17] one imposes the condition

$$u_d = \delta_d, \quad \forall d = (i_0, j_0) \in \partial\Omega, \quad (10)$$

where  $\delta_d(l) \stackrel{\text{def}}{=} 1$  if  $d = l$  and 0 otherwise.

If  $0 \leq w_{ij} \leq 1$  for all  $(i, j) \in \Omega$ , then problem (9) with boundary conditions (10) has a natural probabilistic interpretation. Namely,  $u_{ij}$  represents the probability that a particle undergoing a random walk with absorption will reach the site  $d = (i_0, j_0)$  given that at each site  $\alpha = (\alpha_1, \alpha_2)$  it has a survival probability  $w_\alpha$  for  $\alpha \in \Omega$ . See [16]. We remark that a sufficient condition for  $w_{ij} \in (0, 1)$  is that  $V_{ij} > 0$ . In what follows, we will rely heavily on such an interpretation and the notation presented in [16, 17]. We shall extend some of the results therein to allow more general boundary conditions in the identification of the doping profile. We refer the reader to figure 2 where the different boundary conditions are depicted. In detail, the boundary region  $\partial\Omega$  will be decomposed into two parts,  $\partial\Omega_N$  and  $\partial\Omega_D$ . Such regions have corresponding internal adjacent regions  $\partial\Omega_N^i$  and  $\partial\Omega_D^i$ . On  $\partial\Omega_N$  homogeneous Neumann boundary conditions will be imposed. In this discretized setting, this means that the values of  $u_\alpha$  on pixels  $\alpha \in \partial\Omega_N$  and on the adjacent one  $\alpha' \in \partial\Omega_N^i$  coincide. See figure 2(c). The region  $\partial\Omega_D$  will be further subdivided into two regions  $\Gamma_0$  and  $\Gamma_1$ . On  $\Gamma_0$  we will impose nonhomogeneous Dirichlet data whereas on  $\Gamma_1$  we impose homogeneous Dirichlet data. Here again, for  $l = 0$  or  $1$  we denote by  $\Gamma_l^i$  the interior region adjacent to  $\Gamma_l$ . The measurements correspond to normal derivatives on  $\Gamma_1$ . In other words,  $u_\alpha - u_{\alpha'}$  for  $\alpha \in \Gamma_1$  and  $\alpha' \in \Gamma_1^i$  with  $\alpha'$  adjacent to  $\alpha$ . Since  $u_\alpha = 0$  for  $\alpha \in \Gamma_1$  this corresponds to evaluating  $u_{\alpha'}$  for  $\alpha' \in \Gamma_1^i$ .

The first natural question to be addressed is the well posedness of the direct problem. It is answered by the following.

**Proposition 3.1.** *Given a distribution of values  $w = (w_{i,j})_{1 \leq i,j \leq N} \in (0, 1)^{N \times N}$ , the system of equations in (9) endowed with the boundary conditions*

$$u_\alpha = u_{\alpha'} \quad \text{for } \alpha \in \partial\Omega_N \text{ adjacent to } \alpha' \in \partial\Omega_N^i, \quad (11)$$

$$u_\beta = \delta_d \quad \text{for } \beta \in \Gamma_0, \quad (12)$$

$$u_\gamma = 0 \quad \text{elsewhere on } \partial\Omega \quad (13)$$

has a unique solution for each  $d \in \Gamma_0$ . Furthermore, this solution depends rationally on the components of the array  $w$ .

**Proof.** Let us note that we have a (sparse) system of  $N^2$  equations in the  $N^2$  unknowns  $((u_{ij}))$ . The equations for the sites  $(i, j)$  with  $2 \leq i, j \leq N - 1$  are precisely those given by (9), whereas for the sites  $\alpha' = (i, j) \in \partial\Omega_N^i$  or  $\partial\Omega_D^i$  require us to use the boundary conditions. The variables  $u_\alpha$  on the site  $\alpha$  adjacent to  $\alpha' \in \partial\Omega_N^i$  coincide with  $u_{\alpha'}$ . Thus, the corresponding equation has to be modified accordingly. On the other hand, if  $\alpha' \in \partial\Omega_D^i$  then the value of  $u_\alpha$  must be  $\delta_d(\alpha)$ . On the sites adjacent to the Dirichlet boundary, or on the interior sites, the diagonal element of the matrix representing system (9) is 1. On the sites adjacent to the Neumann boundary, the value of  $w_{ij}$  must be changed to  $w_{ij}/(1 - (w_{ij}/4))$ . In either case, after incorporating the boundary conditions (of mixed Neumann and Dirichlet type) the matrix representing the problem is strictly diagonally dominant. Thus, the system of equations is uniquely solvable, and the solution depends rationally on the coefficients  $w_{ij}$ .  $\square$

**Remark 3.2.** The assumption  $w_{ij} \leq 1$  for all  $i$  and  $j$  is crucial for the above argument. This is ensured, for example, if  $V_{ij} > 0$  for all  $i$  and  $j$ , which in turn can be guaranteed if  $V(x)$  is positive.

**Remark 3.3.** The vanishing Neumann boundary conditions can be recast so as to preserve the probabilistic interpretation of the problem as follows. Suppose that  $(i, j) \in \partial\Omega_N^i$  is adjacent



to  $(i - 1, j) \in \partial\Omega_N$  (similar considerations hold at the other points  $(i, j) \in \partial\Omega_N^i$ ). Then, equation (9) for this site becomes

$$u_{ij} - \frac{w_{ij}}{4 - w_{ij}}(u_{i+1,j} + u_{i-1,j} + u_{i,j+1} + u_{i,j-1}) = 0. \tag{14}$$

**Remark 3.4.** Since the variable  $u_{i-1,j}$  and the coefficient  $w_{i,j}$  do not appear in any other equation in the system, we could reinterpret equation (14) as  $u_{ij} = (w_{ij}^{\text{eff}}/3)(u_{i+1,j} + u_{i-1,j} + u_{i,j+1} + u_{i,j-1})$ , with  $w_{ij}^{\text{eff}} = 3w_{ij}/(4 - w_{ij})$ . Note that  $w_{ij}^{\text{eff}} \in (0, 1)$  if  $w_{ij} \in (0, 1)$ . Thus, for all practical purposes, the equations associated with the Neumann boundary sites could be replaced by equivalent equations with vanishing Dirichlet boundary conditions.

**Remark 3.5.** In [16], a crucial role is played by the probabilistic interpretation of the system of equations (9) in the solution of the inverse problem of the so-called isotropic diffuse tomography problem. See also [27]. In particular, the following Feynman–Kac-type formula holds for a fixed  $d \in \Gamma_0$ :

$$u_{mn} = \sum_{\alpha \in \mathcal{P}_{(m,n)}^d} \prod_{s \in \alpha} t_{\alpha_s}^{\alpha_{s+1}},$$

where  $\mathcal{P}_{(m,n)}^d$  denotes the set of all paths connecting the site  $(m, n)$  to the boundary site  $d$ , and a path  $\alpha$  consists of an ordered set of successively adjacent sites starting at a neighbour to  $(m, n)$  and ending at  $d$ , and  $t_{\alpha_s}^{\alpha_{s+1}}$  denotes the transition probability from the site  $\alpha_s$  to the site  $\alpha_{s+1}$ . Thus,  $t_{\alpha_0}^{\alpha_1} = w_{mn}/4, \dots$

We now turn our attention to the inverse problem. We define the restricted (discrete) DtN map  $\Lambda_{\Gamma_0, \Gamma_1}^w$  which assigns Dirichlet data supported on  $\Gamma_0$  to Neumann measurements on  $\Gamma_1$ . Our next goal is to prove an identification result that is similar in spirit to the main result of [16]. It implies that in the discrete context, and under suitable hypothesis on the potential, one can determine such a potential in the interior of a region defined by the current measurement boundary using voltage-to-current measurements. The larger the boundary  $\Gamma_1$  in figure 2(b), the larger the region where the potential can be uniquely determined from voltage-to-current measurements (provided the total length of  $\Gamma_1$  does not exceed the length of the side of the device). More precisely, we have the following.

**Theorem 3.6.** *For a dense open set of values  $w \in (0, 1)^{N \times N}$ , the map  $\Lambda_{\Gamma_0, \Gamma_1}^w$  uniquely determines the values of  $w_{ij}$  for  $(i, j) \in \Omega$  satisfying  $2 \leq i + j \leq p' + 1$ ,  $2p' \leq N + 1$ , provided the support of the Dirichlet data contains the points  $(N + 1, N), \dots, (N + 1, N - p' + 1)$  and  $p'$  is smaller than the size of one of the sides of  $\Gamma_1$ .*

**Proof.** The argument follows closely that of [16] by proceeding along the diagonals. The  $p$ th diagonal is defined by the sites  $(i, j) \in \Omega$  such that  $i + j = p + 1$ . For instance, the very first diagonal, associated with  $p = 1$ , leads to the equation

$$\widehat{V}_{11}z_{11}^d - (z_{12}^d + z_{10}^d + z_{01}^d + z_{21}^d) = 0, \tag{15}$$

where  $(z_{ij}^d)$  denotes the solution of system (9) with boundary conditions (11)–(13), and Dirichlet data specified as  $\delta_d$  for  $d \in \Gamma_0$ . Furthermore, we shall use the notation  $\widehat{V}_{ij} \stackrel{\text{def}}{=} 4/w_{ij}$ . In this simple case, we see that in equation (15)  $z_{10}^d = z_{01}^d = 0$  and  $z_{11}^d, z_{12}^d, z_{21}^d$  are all boundary measurements, and thus we can recover  $\widehat{V}_{11}$ . The next diagonal ( $p = 2$ ) yields for each detector  $d$ :

$$\widehat{V}_{12}z_{12}^d - (z_{13}^d + z_{11}^d + z_{02}^d + z_{22}^d) = 0, \quad \widehat{V}_{21}z_{21}^d - (z_{22}^d + z_{20}^d + z_{11}^d + z_{21}^d) = 0.$$



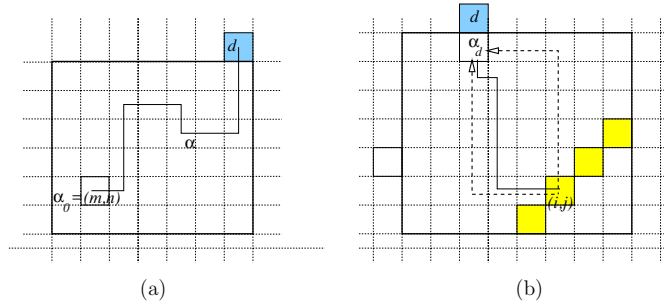


**Figure 3.** Picture (a) shows an example of a path  $\alpha$  connecting an internal point to a boundary point  $d$ . In picture (b), an example of a few minimal length paths connecting an internal point to the point  $\alpha_d$  adjacent to a detector  $d$  is shown.

$$D_p \stackrel{\text{def}}{=} \begin{vmatrix} z_{1,p}^{d_1} & z_{1,p}^{d_2} & z_{1,p}^{d_3} & \cdots & z_{1,p}^{d_{p-1}} & z_{1,p}^{d_p} \\ z_{2,p-1}^{d_1} & z_{2,p-1}^{d_2} & z_{2,p-1}^{d_3} & \cdots & z_{2,p-1}^{d_{p-1}} & z_{2,p-1}^{d_p} \\ \vdots & \vdots & \vdots & \vdots & \vdots & \vdots \\ z_{p-1,2}^{d_1} & z_{p-1,2}^{d_2} & z_{p-1,2}^{d_3} & \cdots & z_{p-1,2}^{d_{p-1}} & z_{p-1,2}^{d_p} \\ z_{p,1}^{d_1} & z_{p,1}^{d_2} & z_{p,1}^{d_3} & \cdots & z_{p,1}^{d_{p-1}} & z_{p,1}^{d_p} \end{vmatrix} \quad (18)$$

does not vanish in the set  $\mathcal{A}$ . Although the technique we employ here is the very same as used in [16], the crucial difference is that in our case the determinant  $D_p$  consists of detectors on the opposite side from where the measurements are being taken. More precisely, we show that the analytic function  $D_p(w)$  is not identically zero in a neighbourhood of  $w = 0$ . Another difference from the situation in [16] is the fact that we have Neumann-type boundary conditions in part of the boundary. This, however, causes no further difficulty in the light of remark 3.3.

To complete the proof, it thus remain to show that if we take all values of  $w_{ij} = \rho$  and let  $\rho \rightarrow 0$ , then under the assumption that  $p \leq p'$ ,  $D_p = A(p)\rho^{L(p)} + \mathcal{O}(\rho^{L(p)+1})$  with  $A(p) \neq 0$  and  $L(p)$  depending only on geometric parameters associated with the size of the grid and the location of the detectors and the diagonal  $p$ . To prove this claim, we start by noting that because of remark 3.5, when  $\rho \rightarrow 0$ , we have  $z_{ij}^d(\rho) = A_{i,j}^{d,p} \rho^{\ell(p,i,j)+1} + \mathcal{O}(\rho^{\ell(p,i,j)+2})$ , where  $\ell(p, i, j)$  is the length of the smallest path connecting the site  $(i, j)$  to the point  $\alpha_d$  in  $\Gamma_0$  adjacent to the detector  $d$ . See figure 3(b). Furthermore,  $A_{i,j}^{d,p}$  denotes the number of paths in the region  $\Omega$  of minimal length  $\ell(p, i, j)$  connecting  $(i, j)$  to  $\alpha_d$ . If we assume that the coordinates of  $\alpha_d = (i', j')$ , then it is easy to check that  $\ell(p, i, j) = |i' - i| + |j' - j|$  and that the number of such paths is given by

$$A_{i,j}^{d,p} = \binom{|i' - i| + |j' - j|}{|i' - i|} = \binom{\ell(p, i, j)}{|i' - i|} = \binom{\ell(p, i, j)}{|j' - j|}. \quad (19)$$

A straightforward combinatorial argument gives that  $A(p) \neq 0$  provided  $2p' \leq N + 1$ .  $\square$

The results presented in this subsection, although following the main ideas in [16], lead to a much more difficult problem than that presented therein. In particular, it is not clear how to go beyond  $p'$ . In fact, the hypothesis that  $2p' \leq N + 1$  is crucial in the above argument,

and although it seems it could be relaxed we do not have a proof of this fact at the present<sup>5</sup>. The treatment of the Neumann boundary conditions and its probabilistic interpretation goes beyond the scope of [16] albeit it shows the power of ideas presented.

#### 4. Numerical approach

In this section, we consider a numerical approach based on level set methods for the inverse doping profile problem in the stationary linearized unipolar case close to equilibrium (see identification problem 2.2). We compare our results with those obtained in [4], where a Landweber–Kaczmarz iterative method was used to reconstruct the doping profile function.

##### 4.1. Framework

As already mentioned in section 2, the main task in this inverse problem consists in the identification of the coefficient  $\gamma$  in the elliptic PDE

$$\operatorname{div}(\gamma \nabla u) = 0 \quad \text{in } \Omega, \quad u = U \quad \text{on } \partial\Omega_D, \quad u_\nu = 0 \quad \text{on } \partial\Omega_N. \quad (20)$$

Thus, we can reduce the inverse doping profile problem to the problem of identifying a piecewise constant function  $\gamma(x)$  in (20) from measurements of the DtN map

$$\begin{aligned} \Lambda_\gamma : H^{3/2}(\partial\Omega_D) &\rightarrow H^{1/2}(\Gamma_1) \\ U &\mapsto \gamma u_\nu|_{\Gamma_1} \end{aligned} \quad (21)$$

(for simplicity we assume  $\gamma(x) \in \{1, 2\}$  a.e. in  $\Omega$ ).

Note that, due to the nature of the boundary conditions related to practical experiments, we have to restrict the domain of definition of the DtN operator to the linear subspace  $D(\Lambda_\gamma) := \{U \in H^{3/2}(\partial\Omega_D); U|_{\Gamma_1} = 0\}$ . Furthermore, the measurements (Neumann data) are only available at  $\Gamma_1$ . This is the essential difference between the parameter identification problem in (20) and the classical inverse problem in *electrical impedance tomography*, namely the fact that both Dirichlet and Neumann data are known only at specific parts of the boundary.

For this particular type of DtN operators, there are so far no analytical results concerning identifiability and, to our knowledge, the few numerical results in the literature are those discussed in [4–6, 13].

In this section, we shall work within the following framework:

- parameter space:  $\mathcal{X} := L^2(\Omega)$ ;
- input (fixed):  $U_j \in H^{3/2}(\partial\Omega_D)$ , with  $U_j|_{\Gamma_1} = 0$ ,  $1 \leq j \leq N$ ;
- output (data):  $Y = \{\Lambda_\gamma(U_j)\}_{j=1}^N \in [L^2(\Gamma_1)]^N =: \mathcal{Y}$ ;
- parameter-to-output map:  $F : D(F) \subset \mathcal{X} \rightarrow \mathcal{Y}$

$$\gamma(x) \mapsto \{\Lambda_\gamma(U_j)\}_{j=1}^N,$$

where the domain of definition of the operator  $F$  is

$$D(F) := \{\gamma \in L^2(\Omega); \gamma_+ \geq \gamma(x) \geq \gamma_- > 0, \text{ a.e. in } \Omega\}$$

(here  $\gamma_-$  and  $\gamma_+$  are appropriate constants). We shall denote noisy data by  $Y^\delta$  and assume that the data error is bounded by  $\|Y - Y^\delta\| \leq \delta$ . Thus, we are able to represent the inverse doping problem in the general form

$$F(\gamma) = Y^\delta. \quad (22)$$

<sup>5</sup> We thank C G Tamm (IMPA) for enlightening discussions on this combinatorial exercise.

For the concrete numerical test performed in this section as well as in [4],  $\Omega \subset \mathbb{R}^2$  is the unit square and the boundary parts are

$$\begin{aligned} \Gamma_1 &:= \{(x, 1); x \in (0, 1)\}, & \Gamma_0 &:= \{(x, 0); x \in (0, 1)\}, \\ \partial\Omega_D &:= \Gamma_0 \cup \Gamma_1, & \partial\Omega_N &:= \{(0, y); y \in (0, 1)\} \cup \{(1, y); y \in (0, 1)\}. \end{aligned}$$

The fixed inputs  $U_j$  vanish at  $\Gamma_1$  and are chosen to be piecewise constant functions on  $\Gamma_0$ .

$$U_j(x) := \begin{cases} 1, & |x - x_j| \leq \delta x, \\ 0, & \text{else,} \end{cases}$$

where the points  $(x_j, 1)$ ,  $j = 1, \dots, N$ , are uniformly distributed along the segment  $\Gamma_0$ .

The next lemma describes some crucial properties of the operator  $F$ , that will be necessary for the analysis of the iterative methods discussed in this paper. Here, only a sketch of the proof of lemma 4.1 is given; for details see [5].

**Lemma 4.1.** *Let the voltages  $\{U_j\}_{j=1}^N$  be chosen in the neighbourhood of  $U = 0$ . The parameter-to-output map  $F$  defined above is well defined and Fréchet differentiable on  $D(F)$ .*

**Proof.** The first statement follows from the well definedness of the  $V$ – $C$  map, cf lemma 2.1. The Fréchet differentiability of  $F$  follows from the differentiability of the  $V$ – $C$  map (see lemma 2.1) together with the differentiability of the map that takes the doping profile  $C$  onto the solution  $(V, u, v)$  of (1).  $\square$

#### 4.2. A competing approach: Landweber–Kaczmarz method

In [4], a Landweber–Kaczmarz method was used to reconstruct the doping profile function. This corresponds to an iterative method of steepest descent type for solving the least-square formulation of the inverse problem.

A simple and robust iterative method to solve the inverse problem (22) is the *Landweber iteration* [7, 8, 10, 18]. This iteration is known to generate a regularization method for the inverse problem, the stopping index playing the role of the regularization parameter (for regularization theory see e.g. [8–10, 29]).

The *Landweber–Kaczmarz method* [20] results from the coupling of the strategies of both the Landweber and the Kaczmarz iterative method. The motivation for this choice of strategy lies in the fact that the data in (22) consist of a vector of measurements  $\{\Lambda_\gamma(U_j)\}_{j=1}^N$  and the principal characteristic of the Kaczmarz method is the minimization, at each iteration step, of a least-square functional that takes into account only one component of this measurement vector. It is worth mentioning that this method has already been successfully applied to *electrical impedance tomography* by Nachman in [25].

To formulate the method, we first need to define the components of the parameter-to-output map:  $F = \{\mathcal{F}_j\}_{j=1}^N$ , where  $\mathcal{F}_j : L^2(\Omega) \supset D(F) \ni \gamma \mapsto \Lambda_\gamma(U_j) \in L^2(\Gamma_1)$ . Now, setting  $Y_j^\delta := \mathcal{F}_j(\gamma^\delta)$ ,  $1 \leq j \leq N$ , the Landweber–Kaczmarz iteration can be written in the form

$$\gamma_{k+1}^\delta = \gamma_k^\delta - \mathcal{F}'_k(\gamma_k^\delta)^* (\mathcal{F}_k(\gamma_k^\delta) - Y_k^\delta), \tag{23}$$

for  $k = 1, 2, \dots$ , where we adopted the notation  $\mathcal{F}_k := \mathcal{F}_j$ ,  $Y_k^\delta := Y_j^\delta$ , whenever  $k = iN + j$ , and  $i = 0, 1, \dots$  and  $j = 1, \dots, N$ .

Note that each step of the Landweber–Kaczmarz method consists of one Landweber iterative step with respect to the  $j$ th component of the residual in (22). These Landweber steps are performed in a cyclic way, using the components of the residual  $\mathcal{F}_j(\gamma) - Y_j^\delta$ ,  $1 \leq j \leq N$ , one at a time.

### 4.3. A level set approach

In this paper, we propose a level set type method to approximate the solution of (20). In the following, the function spaces  $\mathcal{X}, \mathcal{Y}$  as well as the operators  $F, \Lambda_\gamma$  and also the sets  $\Omega, \partial\Omega_D, \partial\Omega_N, \Gamma_0, \Gamma_1$  are the same as above. We assume, however, that only one measurement is given, i.e., only one pair of voltage–current data is available for the reconstruction. This assumption corresponds to the choice  $N = 1$  in the definition of the space  $\mathcal{Y}$ .

Our numerical approach is based on the level set method introduced in [14, 21]. According to this strategy, one represents the unknown P–N junction by the zero level set of an  $H^1$ -function  $\phi : \Omega \rightarrow \mathbb{R}$ , in such a way that  $\phi(x) > 0$  if  $\gamma(x) = 2$  and  $\phi(x) < 0$  if  $\gamma(x) = 1$ . Starting from some initial guess  $\phi_0 \in H^1(\Omega)$ , one solves the Hamilton–Jacobi equation

$$\frac{\partial \phi}{\partial t} + V \nabla \phi = 0, \quad (24)$$

where  $V = -v \nabla \phi / |\nabla \phi|^2$  and the velocity  $v$  solves

$$\begin{cases} (\Delta - I)v = \frac{\delta(\phi(t))}{|\nabla \phi(t)|} \left[ F'(\chi(t))^*(F(\chi(t)) - Y^\delta) - \beta \nabla \cdot \left( \frac{\nabla P(\phi)}{|\nabla P(\phi)|} \right) \right] & \text{in } \Omega, \\ \frac{\partial v}{\partial \nu} = 0 & \text{on } \partial\Omega. \end{cases} \quad (25)$$

Here,  $\alpha > 0$  is a regularization parameter and  $\chi = \chi(x, t)$  is the projection of the level set function  $\phi(x, t)$  defined by

$$\chi(x, t) = P(\phi(x, t)) := \begin{cases} 2, & \text{if } \phi(x, t) > 0, \\ 1, & \text{if } \phi(x, t) < 0. \end{cases}$$

In [14, 21], this level set method was used to reconstruct inclusions  $D \subset\subset \Omega$ . Note that, in our case, the set  $D$  corresponds to the P-region (see figure 1) and the condition  $\overline{D} \subset \Omega$  is not satisfied. This fact, however, does not affect the derivation of the Hamilton–Jacobi equation (24). Moreover, it does not affect the derivation of the boundary conditions for the elliptic problem (25) either.

The family  $\chi(\cdot, t)$  approximates the doping profile  $\gamma(\cdot)$  as  $t \rightarrow \infty$ . This follows from the fact that the solution  $\phi(\cdot, t)$  of (24) converges to the minimum of the Tikhonov functional

$$\mathcal{G}_\alpha(\phi) := \|F(P(\phi)) - Y^\delta\|_{\mathcal{Y}}^2 + \alpha(2\beta|P(\phi)|_{\text{BV}} + \|\phi - \phi_0\|_{H^1(\Omega)}^2) \quad (26)$$

as  $t \rightarrow \infty$ , for each regularization parameter  $\alpha > 0$  ( $\beta > 0$  is fixed). See [14, definition 2.2] for the precise definition of a minimizer of  $\mathcal{G}_\alpha(\phi)$ .

The next lemma corresponds to specific results selected from [14]. It allows a better understanding of the least-square problem behind the level set formulation and also analytically substantiates the numerical results presented in the following.

**Lemma 4.2** (stability, convergence and well posedness).

- Let  $Y^\delta = Y$  (noiseless case) and let  $\phi_\alpha$  be a minimizer of  $\mathcal{G}_\alpha$ . Then, for every sequence  $\{\alpha_k\}_{k \in \mathbb{N}}$  converging to zero, there exists a subsequence  $\{\alpha_{k(l)}\}_{l \in \mathbb{N}}$ , such that  $\{\phi_{\alpha_{k(l)}}\}_{l \in \mathbb{N}}$  is strongly convergent. Moreover, the limit is a minimal norm solution of (22).
- Let  $\|Y^\delta - Y\|_{\mathcal{Y}} \leq \delta$ . If  $\alpha = \alpha(\delta)$  satisfies  $\lim_{\delta \rightarrow 0} \alpha(\delta) = 0$  and  $\lim_{\delta \rightarrow 0} \frac{\delta^2}{\alpha(\delta)} = 0$ , then, for a sequence  $\{\delta_k\}_{k \in \mathbb{N}}$  converging to 0, the sequence  $\phi_{\alpha(\delta_k)}$  converges to a minimal norm solution of (22).
- For any given  $\phi_0 \in H^1(\Omega)$ , the functional  $\mathcal{G}_\alpha$  attains a minimizer.

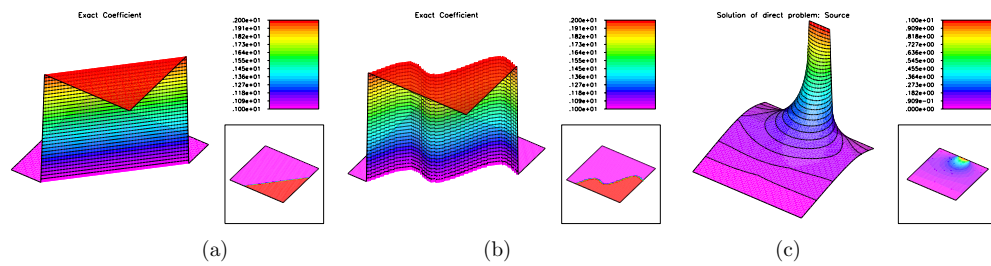


**Figure 4.** Pictures (a) and (b) show the doping profiles to be reconstructed in the two different experiments for the level set method. In picture (c), the problem data are shown: the source  $U(x)$  appears as the Dirichlet boundary condition at  $y = 1$  ( $\Gamma_0$  is the upper-right edge). The corresponding current is measured at the contact  $\Gamma_1$  (lower-left edge), where  $U(x)$  is assumed to vanish.

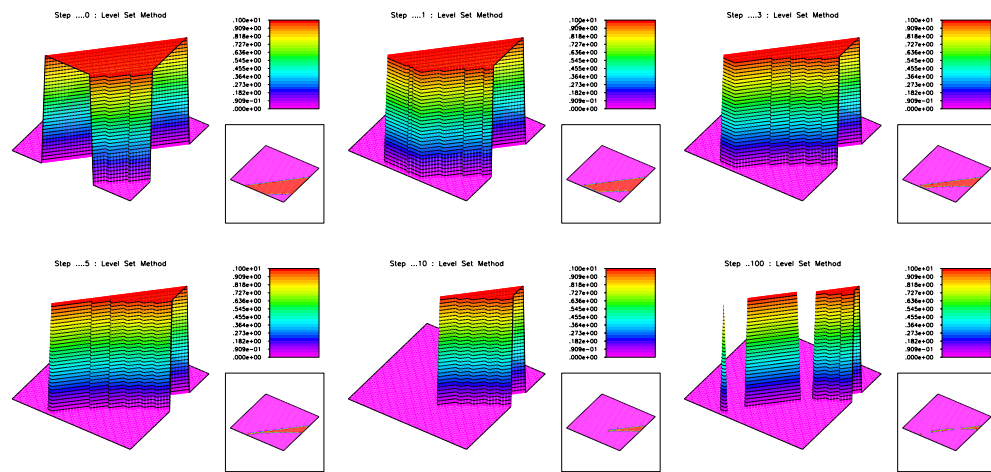


**Figure 5.** First numerical experiment (linear P–N junction): evolution of the iteration error for the level set method and exact data.

**Remark 4.3.** (level set algorithm). For the reader’s convenience, we briefly describe the level set algorithm related to (24), (25). Here,  $P_\varepsilon$  is the approximation defined in [14, section 2] for the operator  $P$ . The adjoint operator  $(F')^*$  as well as its evaluation on a given vector is derived in [4, section 4].

1. Evaluate the residual  $r_k := F(P_\varepsilon(\phi_k)) - Y^\delta$ .
2. Evaluate  $w_k := F'(P_\varepsilon(\phi_k))^*(r_k)$ .
3. Evaluate  $v_k \in H^1(\Omega)$ , satisfying

$$\begin{aligned}
 (\Delta - I)v_k &= P'_\varepsilon(\phi_k) \left( w_k - \beta P'_\varepsilon(\phi_k) \nabla \cdot \left( \frac{\nabla P_\varepsilon(\phi_k)}{|\nabla P_\varepsilon(\phi_k)|} \right) \right) \quad \text{in } \Omega, \\
 \partial v_k / \partial \nu &= 0 \quad \text{on } \partial\Omega.
 \end{aligned}$$

4. Update the level set function  $\phi_{k+1} = \phi_k + v_k$ .

We conclude this section presenting two different numerical experiments concerning the identification problem in (20).

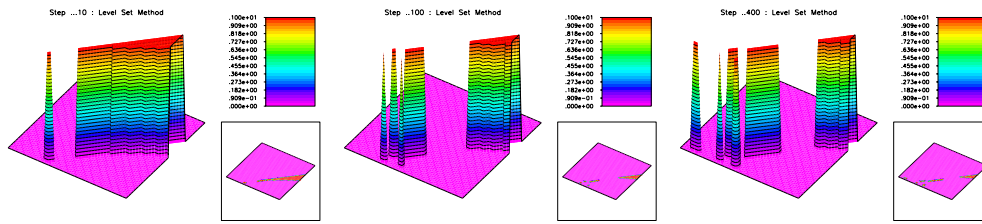


**Figure 6.** First numerical experiment (linear P–N junction): evolution of the iteration error for the level set method and data with 10% random noise.

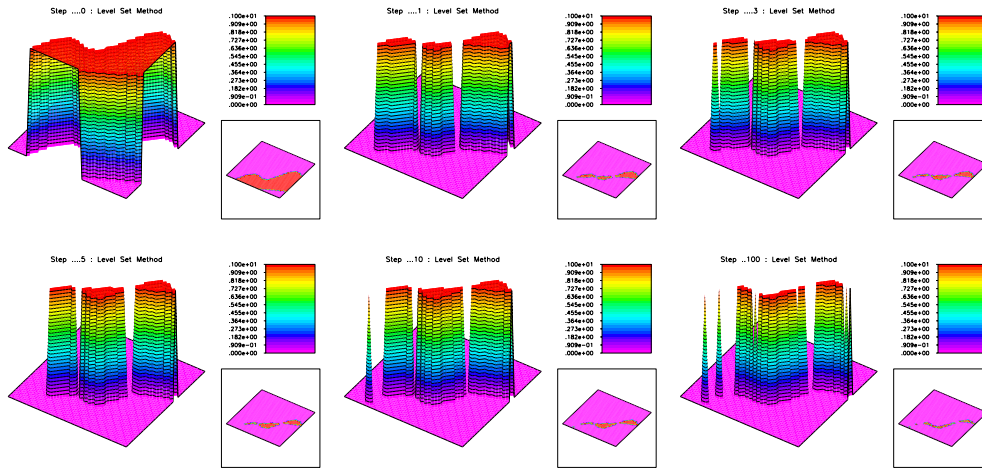


**Figure 7.** Second numerical experiment (analytical P–N junction): evolution of the iteration error for the level set method and exact data.

- The first one, for comparison purposes, corresponds to the identification problem considered in [4] (linear P–N junction; see figure 4(a)). Initially, we implemented the level set method for the case of exact data (see figure 5). Note that the first picture (top left) corresponds to the initial guess. In a second run, we added 10% random noise to the exact data and repeated the experiment (see figure 6).
- In the second experiment, we try to identify a P–N junction parameterized by an analytical function (see figure 4(b)). Exact data are used for the reconstruction (see figure 7).

The voltage–current data pair in the first experiment corresponds to the boundary values of the function shown in figure 4(c). This picture shows the solution of (20) for a typical source  $U(x)$ .

## 5. Final comments and conclusions

### 5.1. A priori knowledge of the doping profile

Due to the choice of  $\Omega$ ,  $\partial\Omega_D$  and  $\partial\Omega_N$  meet at angles of  $\pi/2$ . Thus, the solutions of the mixed boundary value problems in the Landweber–Kaczmarz iteration are not in  $H^2(\Omega)$  (see [15] for details). Due to this lack of regularity, the implementation turns out to be very unstable. In order to bypass this instability, in [4] the authors made the additional assumption that the



doping profile is known in a thin strip close to  $\partial\Omega_D$ . Therefore, only the values of  $\gamma(x)$  at a subdomain  $\tilde{\Omega} \subset \subset \Omega$  had to be reconstructed.

Differently from the Landweber–Kaczmarz approach in [4], the level set method does not require the assumption that the doping profile is known in some strip close to  $\partial\Omega_D$ . For this level set approach, only the knowledge of the doping profile at  $\Gamma_1$  is required in order to obtain a stable performance of the method. This weaker assumption agrees with the physical experiment, since we need to know  $\gamma$  at  $\Gamma_1$  in order to implement the DtN map in (21).

### 5.2. Amount of data and quality of the reconstruction

We now comment on the amount of information used in the identification. In [4], the Landweber–Kaczmarz method was implemented using different amount of data, i.e., a different number of data voltage–current pairs. In one of the experiments, a single pair of data was used. In this case, the Landweber–Kaczmarz method reduces to the classical Landweber iteration.

It is worth noting that the amount of available data strongly influences the quality of the reconstruction in the Landweber–Kaczmarz method. However, observing the results in [4], no matter how many voltage–current pairs are available, it does not allow a proper determination of the P–N junction.

What concerns the quality of the reconstruction of the P–N junction, the level set approach considered in this paper brings much better results. In particular, if one takes into account that only one pair of voltage–current data is used.

A possible explanation for the different performance of these methods is the fact that the Landweber–Kaczmarz approach does not take into account the assumption that the coefficient  $\gamma$  in (20) for such an application is a piecewise constant function. The Landweber–Kaczmarz method tries to identify a real function defined on  $\Omega$ , which is a much more complicated object than the original unknown curve (the P–N junction). Due to the nature of the level set approach, it incorporates in a natural way the assumption that  $\gamma$  is piecewise constant in  $\Omega$ .

### 5.3. Numerical effort

Next, we compare the numerical effort required for the implementation of the Landweber–Kaczmarz and the level set method. If both methods are implemented using a single pair of voltage–current data, each step of the Landweber–Kaczmarz method requires the solution of two mixed boundary value problems (BVPs), while each level set step requires the solution of three BVPs. However, the use of nine pairs of data (as in [4]) requires the solution of 18 BVPs in each cycle of the Landweber–Kaczmarz method. This observation agrees with our numerical tests, where we observed that a level set step is about ten times faster than a Landweber–Kaczmarz cycle for nine pairs of voltage–current data.

It is worth noting that not only the numerical effort for each step of the level set method is smaller than the effort for a Landweber–Kaczmarz cycle, but also the total number of steps required to obtain a good approximation is smaller than the total number of cycles. In [4], the iteration was stopped after 5000 cycles (for both exact and noisy data of 10%). This numerical test corresponds to our first experiment, where we needed 100 steps in the case of exact data and 400 steps for noisy data.

## Acknowledgments

The work of AL was partially supported by the Brazilian National Research Council CNPq, grants 305823/03-5 and 478099/04-5. JPZ acknowledges financial support from CNPq, grants 302161/03-1 and 474085/03-1, and from Prosul program, grant 490300. PAM

acknowledges support from the Austrian National Science Foundation FWF through his Wittgenstein Award 2000.

## References

- [1] Astala K and Päiväranta L 2006 Calderón's inverse conductivity problem in the plane *Ann. Math.* **163** 265–99
- [2] Borcea L 2002 Electrical impedance tomography *Inverse Problems* **18** R99–136
- [3] Bukhgeim A and Uhlmann G 2002 Recovering a potential from partial Cauchy data *Commun. Part. Diff. Eqns* **27** 653–68
- [4] Burger M, Engl H W, Leitão A and Markowich P A 2004 On inverse problems for semiconductor equations *Milan J. Math.* **72** 273–314
- [5] Burger M, Engl H W, Markowich P A and Pietra P 2001 Identification of doping profiles in semiconductor devices *Inverse Problems* **17** 1765–95
- [6] Burger M, Engl H W and Markowich P 2002 Inverse doping problems for semiconductor devices *Recent Progress in Computational and Applied PDEs* ed T F Chan *et al* (Dordrecht: Kluwer/Plenum) pp 27–38
- [7] Deuffhard P, Engl H W and Scherzer O 1998 A convergence analysis of iterative methods for the solution of nonlinear ill-posed problems under affinity invariant conditions *Inverse Problems* **14** 1081–106
- [8] Engl H W, Hanke M and Neubauer A 1996 *Regularization of Inverse Problems* (Dordrecht: Kluwer) (Paperback, 2000)
- [9] Engl H W, Kunisch K and Neubauer A 1989 Convergence rates for Tikhonov regularization of nonlinear ill-posed problems *Inverse Problems* **5** 523–40
- [10] Engl H W and Scherzer O 2000 Convergence rates results for iterative methods for solving nonlinear ill-posed problems *Surveys on Solution Methods for Inverse Problems* ed D Colton *et al* (Vienna: Springer) pp 7–34
- [11] Fang W and Ito K 1992 Identifiability of semiconductor defects from LBIC images *SIAM J. Appl. Math.* **52** 1611–26
- [12] Fang W and Ito K 1994 Reconstruction of semiconductor doping profile from laser-beam-induced current image *SIAM J. Appl. Math.* **54** 1067–82
- [13] Fang W, Ito K and Redfern D A 2002 Parameter identification for semiconductor diodes by LBIC imaging *SIAM J. Appl. Math.* **62** 2149–74
- [14] Frühauf F, Scherzer O and Leitão A 2005 Analysis of regularization methods for the solution of ill-posed problems involving discontinuous operators *SIAM J Numer. Anal.* **43** 767–86
- [15] Grisvard P 1985 *Elliptic Problems in Nonsmooth Domains* (London: Pittman)
- [16] Grünbaum A F 1992 Diffuse tomography: the isotropic case *Inverse Problems* **8** 409–19
- [17] Grünbaum F A and Zubelli J P 1992 Diffuse tomography: computational aspects of the isotropic case *Inverse Problems* **8** 421–33
- [18] Hanke M, Neubauer A and Scherzer O 1995 A convergence analysis of the Landweber iteration for nonlinear ill-posed problems *Numer. Math.* **72** 21–37
- [19] Isakov V 1998 *Inverse problems for partial differential equations Applied Mathematical Sciences* (New York: Springer)
- [20] Kowar R and Scherzer O 2002 Convergence analysis of a Landweber–Kaczmarz method for solving nonlinear ill-posed problems *Ill-Posed and Inverse Problems* ed S I Kabanikhin *et al* (Boston, MA: VSP) pp 253–70
- [21] Leitão A and Scherzer O 2003 On the relation between constraint regularization, level sets, and shape optimization *Inverse Problems* **19** L1–11
- [22] Markowich P A 1986 *The Stationary Semiconductor Device Equations* (Vienna: Springer)
- [23] Markowich P A, Ringhofer C A and Schmeiser C 1990 *Semiconductor Equations* (Vienna: Springer)
- [24] Nachman A I 1996 Global uniqueness for a two-dimensional inverse boundary value problem *Ann. Math.* **143** 71–96
- [25] Natterer F 1986 *The Mathematics of Computerized Tomography* (Stuttgart: Teubner/Wiley) (Reprinted in *SIAM Classics in Applied Mathematics* 1991)
- [26] Selberherr S 1984 *Analysis and Simulation of Semiconductor Devices* (New York: Springer)
- [27] Svaiter B F and Zubelli J P 2001 Convexity for the diffuse tomography model *Inverse Problems* **17** 729–38
- [28] van Roosbroeck W R 1950 Theory of flow of electrons and holes in germanium and other semiconductors *Bell Syst. Tech. J.* **29** 560–607
- [29] Tikhonov A N and Arsenin V Y 1977 *Solutions of Ill-Posed Problems* (New York: Wiley)